CX_3CR1 Deficiency Does Not Influence Trafficking of Adipose Tissue Macrophages in Mice With Diet-Induced Obesity

David L. Morris[1], Kelsie E. Oatmen[1,2], Tianyi Wang[1,2], Jennifer L. DelProposto[1] and Carey N. Lumeng[1,3]

Adipose tissue macrophages (ATMs) accumulate in fat during obesity and resemble foam cells in atherosclerotic lesions, suggesting that common mechanisms underlie both inflammatory conditions. CX_3CR1 and its ligand fractalkine/CX_3CL1 contribute to macrophage recruitment and inflammation in atherosclerosis, but their role in obesity-induced adipose tissue inflammation is unknown. Therefore, we tested the hypothesis that CX_3CR1 regulates ATM trafficking to epididymal fat and contributes to the development of adipose tissue inflammation during diet-induced obesity. *Cx_3cl1* and *Cx_3cr1* expression was induced specifically in epididymal fat from mice fed a high-fat diet (HFD). CX_3CR1 was detected on multiple myeloid cells within epididymal fat from obese mice. To test the requirement of CX_3CR1 for ATM trafficking and obesity-induced inflammation, *$Cx_3cr1^{+/GFP}$* and *$Cx_3cr1^{GFP/GFP}$* mice were fed a HFD. Ly-$6c^{Low}$ monocytes were reduced in lean *$Cx_3cr1^{GFP/GFP}$* mice; however, HFD-induced monocytosis was comparable between strains. Total ATM content, the ratio of type 1 ($CD11c^+$) to type 2 ($CD206^+$) ATMs, expression of inflammatory markers, and T-cell content were similar in epididymal fat from obese *$Cx_3cr1^{+/GFP}$* and *$Cx_3cr1^{GFP/GFP}$* mice. *Cx_3cr1* deficiency did not prevent the development of obesity-induced insulin resistance or hepatic steatosis. In summary, our data indicate that CX_3CR1 is not required for the recruitment or retention of ATMs in epididymal adipose tissue of mice with HFD-induced obesity even though CX_3CR1 promotes foam cell formation. This highlights an important point of divergence between the mechanisms regulating monocyte trafficking to fat with obesity and those that contribute to foam cell formation in atherogenesis.

Obesity (2012) **20,** 1189–1199. doi:10.1038/oby.2012.7

INTRODUCTION

The development of metabolic syndrome and type 2 diabetes is linked to obesity-induced inflammation in visceral adipose tissue (1). Adipose tissue contains a wide variety of leukocytes (e.g., monocytes, macrophages, mast cells, B and T lymphocytes, and neutrophils), but adipose tissue macrophages (ATMs) are thought to be the major effectors of adipose tissue inflammation (2). In lean mice and humans, visceral fat contains predominantly resident (type 2) ATMs that express markers of alternative (M2) macrophage activation (3–5). However, obesogenic diets (Western or high fat) promote quantitative and qualitative changes in ATM subtypes within fat that are associated with measures of inflammation and insulin resistance (5–7). Specifically, high-fat diets (HFD) promote the recruitment of inflammatory (type 1) ATMs that express the marker CD11c, produce pro-inflammatory cytokines, and cluster around dead adipocytes (8,9). Ablation of $CD11c^+$ ATMs in obese mice reduces inflammation and improves insulin sensitivity, establishing a link between the infiltration of type 1 ATMs and metabolic disease (10). However, the mechanisms by which monocytes/ATMs traffic to adipose tissue during steady state and in response to obesity are incompletely understood and a key question in the field.

The accumulation of inflammatory type 1 ATMs in obese visceral fat mimics foam cell accumulation in atherosclerotic vessels (11,12). Moreover, both foam cell formation and recruitment of type 1 ATMs to fat are dependent upon the chemokine receptor CCR2 and its ligand CCL2/MCP1 (13–16). Recent studies have also demonstrated that other inflammatory mediators commonly found in atherosclerotic plaques (e.g., T cells, B cells, and mast cells) are enriched in obese adipose tissue as well (17–19). Collectively, these findings have led to the generally held idea that factors which regulate foam cell formation during atherogenesis may be synonymous with those that promote ATM accumulation and adipose tissue inflammation with obesity.

In addition to CCR2, the fractalkine receptor CX_3CR1 regulates monocyte trafficking to sites of inflammation and plays

[1]Department of Pediatrics and Communicable Diseases, University of Michigan, Ann Arbor, Michigan, USA; [2]Literature, Science and Arts Program, University of Michigan, Ann Arbor, Michigan, USA; [3]Department of Molecular and Integrative Physiology, University of Michigan Medical School, Ann Arbor, Michigan, USA. Correspondence: Carey N. Lumeng (clumeng@umich.edu)

Received 31 August 2011; accepted 5 January 2012; advance online publication 2 February 2012. doi:10.1038/oby.2012.7

a critical role in foam cell formation. CX_3CR1 is differentially expressed on two distinct subsets of blood monocytes. In mice, resident monocytes ($CD115^+$ Ly-$6c^-$ ($Gr\text{-}1^-$) $7/4^{Mid}$ CX_3CR1^{High} $CCR2^-$) are long-lived, patrolling leukocytes that give rise to tissue macrophages under homeostatic conditions; conversely, inflammatory monocytes ($CD115^+$ Ly-$6c^{High}$ ($Gr\text{-}1^+$) $7/4^{High}$ CX_3CR1^{Mid} $CCR2^{High}$ $CD62L^+$) are short-lived and migrate rapidly from the circulation into inflamed tissues (20,21). CX_3CR1 enhances Ly-$6c^{High}$ monocyte adhesion to endothelial cells (22), but also promotes the survival of circulating Ly-$6c^{Low}$ monocytes (23). Disruption of either CX_3CR1 or it ligand (fractalkine/CX_3CL1) attenuates macrophage accumulation and inflammation in mice models of atherosclerosis (24–26). Notably, CX_3CR1/CX_3CL1 synergizes with CCR2/CCL2 to maximize foam cell formation and the inflammatory response during atherogenesis (14,27,28). Whether CX_3CR1/CX_3CL1 plays a similar role in ATM accumulation is unknown.

Recently, fractalkine/CX_3CL1 has been shown to be elevated in plasma and adipose tissue from obese patients (29), suggesting that CX_3CL1/CX_3CR1 may also be involved in adipose tissue inflammation. Based on this finding and the importance of CX_3CR1 and CX_3CL1 in monocyte trafficking and foam cell formation, we examined the hypothesis that CX_3CR1 regulates ATM recruitment during HFD-induced obesity. Unlike atherosclerosis models, our data indicate that CX_3CR1 is not required for trafficking of resident type 2 ATMs or for obesity-induced accumulation of inflammatory type 1 ATMs. Ultimately, we found that *Cx_3cr1* deficiency does not impact HFD-induced insulin resistance or liver steatosis in mice. These findings suggest that monocytes/macrophages employ fundamentally different mechanisms to accumulate in adipose tissue during obesity as compared to atherosclerotic vessels.

METHODS AND PROCEDURES

Mice and diets

C57BL/6J mice and B6.129P-*$Cx_3cr1^{tm1Litt}$/J* (*$Cx_3cr1^{GFP/GFP}$*) mice (C57BL/6 background) were purchased from The Jackson Laboratory, Bar Harbor, ME. In *$Cx_3cr1^{GFP/GFP}$* mice, both endogenous *Cx_3cr1* alleles are disrupted by an enhanced green fluorescent protein (GFP) reporter gene. Male *$Cx_3cr1^{GFP/GFP}$* mice were crossed with female C57BL/6 mice to generate *$Cx_3cr1^{+/GFP}$* hemizygous mice. Subsequently, male *$Cx_3cr1^{GFP/GFP}$* mice were crossed with female *$Cx_3cr1^{+/GFP}$* mice to generate *$Cx_3cr1^{+/GFP}$* and *$Cx_3cr1^{GFP/GFP}$* littermates. Beginning at 8–9 weeks of age, *$Cx_3cr1^{+/GFP}$* and *$Cx_3cr1^{GFP/GFP}$* male mice were fed a HFD consisting of 60% calories from fat (Research Diets, New Brunswick, NJ) to induce obesity. Lean control mice were fed normal diets (ND) consisting of 4.5% calories from fat (LabDiet 5002; PMI Nutrition International, St Louis, MO). Mice were housed in a specific pathogen-free facility on a 12-h light/12-h dark cycle and given free access to food and water. All animal use was in compliance with the Institute of Laboratory Animal Research Guide for the Care and Use of Laboratory Animals. Animal procedures were approved by the University Committee on Use and Care of Animals (UCUCA) at the University of Michigan.

RNA extraction and real-time reverse transcription-PCR analysis

Tissues were isolated, frozen in liquid nitrogen, and stored at −80 °C. Total RNA was isolated from adipose tissue, isolated adipocytes, and stromal vascular cells (SVCs) using the RNeasy Lipid Tissue Kit (Qiagen, Valencia, CA). In all cases, a DNase digestion step was performed according to the manufacturer's instructions. cDNA was generated from 0.5–1.0 mg total RNA using High Capacity cDNA Reverse Transcription Kits (Applied Biosystems, Carlsbad, CA). Real-time PCR analysis was performed using Power SYBR Green PCR Master Mix (Applied Biosystems) and the StepOnePlus System (Applied Biosystems). *Arbp* expression was used as the internal control for data normalization. DNA sequences for the PCR primers used for real-time PCR are provided (**Supplementary Table S1** online). Samples were assayed in duplicate and relative expression was determined using the $2^{-\Delta\Delta CT}$ method.

3T3L1 cell culture

3T3-L1 fibroblasts were propagated and differentiated into adipocytes as previously described (8). After differentiation (day 6), adipocytes were cultured at 37 °C and 8% CO_2 in Dulbecco's modified Eagle's medium containing either 5 mmol/l or 25 mmol/l glucose and 10% fetal bovine serum and media was replaced daily. Adipocytes were used 10 days after differentiation.

Bone marrow-derived macrophage culture

Bone marrow cells were harvested from C57BL/6 male mice and plated onto 12-well culture dishes at 1×10^6 cells/ml. Cells were grown in Dulbecco's modified Eagle's medium supplemented with 20% L929 conditioned medium and 10% heat-inactivated fetal bovine serum for 7 days before use.

Microscopy

Immunofluorescence microscopy was performed as previously described (8). Mice were perfused with 1% paraformaldehyde before tissues were dissected. Adipose tissue samples were incubated en bloc in primary and secondary antibodies in phosphate buffered saline (PBS) containing 5% bovine serum albumin (BSA). For intracellular staining with anti-GFP or anti-Caveolin antibodies, samples were stained in PBS/5% BSA containing 0.3% Triton X-100 (PBS-T/BSA). Adipose tissue and liver samples were fixed in 10% formalin overnight for histology. Paraffin sections were prepared and stained with hematoxylin and eosin. An Olympus DP72 camera attached to an Olympus inverted microscope was used to capture epifluorescence and hematoxylin and eosin images. Confocal images were captured with an Olympus FluoView microscope (60× water immersion objective) and processed with FluoView software (Olympus, Tokyo, Japan). Confocal images were pseudocolored in FluoView or Image J (National Institutes of Health, Bethesda, MD). Image J software was used to generate composite images.

Antibodies

Fc-block (anti-CD16/CD32) and anti-F4/80, anti-Mac2, anti-CD115-PE, F4/80-PerCP5.5, Ly-6c-PerCP5.5, CD11c-PE-Cy7, Ly-6g-APC-Cy7, and CD11b-APC-Cy7 antibodies were from eBioscience, San Diego, CA. The CD206-APC antibody was from AbD Serotec, Raleigh, NC. The anti-GFP antibody was from AbCam, Cambridge, MA. Anti-Caveolin antibody was from BD Biosciences, San Jose, CA. Isolectin-Alexa Fluor 647 and Alexa Fluor-488, -568, and -647 conjugated secondary antibodies were from Invitrogen, Carlsbad, CA.

Isolation of blood leukocytes

Mice were restrained and blood (50 ml) was collected from the tail vein in heparinized micro-hematocrit capillary tubes (Fisher, Pittsburgh, PA). Red blood cells were lysed in 1 ml H_2O and blood leukocytes were resuspended in PBS/0.5% BSA before staining.

Isolation of adipose tissue SVCs

Mice were perfused with 10 ml PBS before fat pads were excised and minced in Hanks' Balanced Salt Solution (HBSS; Invitrogen) containing calcium, magnesium and 0.5% BSA. Collagenase (Type II; Sigma-Aldrich, St Louis, MO) was added to a final concentration of

1 mg/ml and tissue suspensions were incubated at 37 °C for 20–30 min with constant shaking. The resulting cell suspensions were filtered through a 100-μm filter and centrifuged at 500 *g* for 10 min to separate floating adipocytes from the SVC-containing pellet. For some experiment, SVCs were plated on cell culture dishes at 1×10^6 cells per ml. After 2–3 h, SVCs were rinsed with PBS and fresh Dulbecco's modified Eagle's medium containing 10% heat-inactivated fetal bovine serum was added. Cultured SVCs were used within 48 h of isolation. For RNA isolation, SVCs and isolated adipocytes were homogenized in QIAzol Lysis Reagent (Qiagen). For flow cytometry, SVCs were incubated in 0.5 ml RBC lysis buffer for 5 min at room temperature and then resuspended in PBS/0.5% BSA.

Flow cytometry

Blood leukocytes and SVCs (10^7/ml) were incubated in Fc Block (rat anti-mouse CD16/CD32; eBioscience) for 15 min on ice. Cells were stained with the indicated antibodies for 30 min at 4 °C in the dark. Stained cells were washed twice in PBS and fixed in 0.1% paraformaldehyde. Cells were analyzed using a FACSCanto II Flow Cytometer (BD Biosciences) and WEASEL flow cytometry software (version 3.0.1 for Mac OSX; The Walter and Eliza Hall Institute).

Identification of crown-like structures

Adipose tissue samples were stained with anti-Caveolin and anti-Mac2 antibodies in PBS-T/BSA. Samples were imaged using a 20× objective lens.

Glucose and insulin tolerance tests

Mice were fasted for 6 h (10:00 AM–4:00 PM) before glucose tolerance tests and insulin tolerance tests. For glucose tolerance tests, D-glucose (0.7 g/kg of body weight) was administered by intraperitoneal injection. For insulin tolerance tests, human insulin (1 unit Humulin R (Eli Lilly, Indianapolis, IN) per kg of body weight) was delivered intraperitoneally. Blood glucose concentrations (mg/dl) were measured 0, 15, 30, 45, 60, 90, and 120 min after injection using a glucometer (One Touch Ultra; Lifescan, Milpitas, CA).

Serum analysis

Blood samples were collected from the tail vein of restrained mice in serum-separating tubes (BD). Serum samples were frozen at −80 °C until analysis. Plasma insulin levels were measured using a mouse insulin ELISA kit (Crystal Chem, Downers Grove, IL).

Hepatic triglyceride content

Livers were weighed, snap frozen in liquid nitrogen, and stored at −80 °C. Frozen liver samples (200 mg) were thawed, homogenized in buffer A (50 mmol/l Tris, 5 mmol/l EDTA, 30 mmol/l mannitol), and mixed with 250 mmol/l KOH. Lipids were extracted using chloroform/methanol (2:1). Samples were dried overnight at room temperature and resuspended in buffer B (60% butanol/33% Triton X-114/6.6% methanol). Total triglycerides were quantified using a Triglyceride Assay Kit (Sigma) and values were normalized to liver tissue mass.

Statistical analysis

Data are expressed as mean ± s.e.m. GraphPad Prism software (version 5.01; GraphPad Software, La Jolla, CA) was used for statistical analysis. Differences between two groups were determined using unpaired, two-tailed Student's *t*-test. Where appropriate, data was analyzed by two-way ANOVA to test relative contributions of diet and genotype. $P \leq 0.05$ was considered significant.

RESULTS

Cx_3cl1 and Cx_3cr1 expression is increased in epididymal fat in mice with HFD-induced obesity

Cx_3cl1 and *Cx_3cr1* gene expression was measured in epididymal (visceral) and inguinal (subcutaneous) adipose depots from male C57BL/6J mice fed a ND (4.5% fat) or a HFD (60% fat) for 20 weeks to induce obesity. *Cx_3cl1* and *Cx_3cr1* expression was induced in epididymal adipose tissue in obese mice but not in inguinal fat, whereas HFD induced *Ccl2* and *Ccr2* gene expression in both depots (**Figure 1a**). *Cx_3cl1* expression was induced in adipocytes, but repressed in SVCs during HFD-induced obesity (**Figure 1b**). Consistent with this, *Cx_3cl1* expression was induced by lipopolysaccharide in small 3T3-L1 adipocytes generated by culturing differentiated cells in low glucose (5 mmol/l) containing media (**Figure 1c**). However, lipopolysaccharide-induced *Cx_3cl1* expression was elevated more dramatically in large adipocytes grown in high glucose (25 mmol/l) concentrations (**Figure 1c**). In contrast, lipopolysaccharide failed to augment *Cx_3cl1* expression in either bone marrow-derived macrophages (BMMφ) or cultured SVCs (**Figure 1d**). These data indicate that adipocytes in visceral fat are the primary regulated source of CX_3CL1 from obese mice, which is consistent with the work of Shah *et al.* (29). However, our data also suggest that hyperglycemia, adipocyte hypertrophy, or both may synergize with inflammatory signals to promote *Cx_3cl1* expression in adipocytes during HFD-induced obesity.

CX_3CR1 is expressed on multiple $CD11b^+$ SVCs in epididymal fat from mice

CX_3CR1 is expressed on resident type 2 (M2) ATMs in lean mice (4), but its distribution in visceral fat during obesity has not been characterized. Therefore, we examined the distribution of CX_3CR1-expressing cells in epididymal fat from *$Cx_3cr1^{+/GFP}$* hemizygous knock-in mice that had been fed a HFD for 12–20 weeks. In epididymal fat from obese *$Cx_3cr1^{+/GFP}$*, the GFP reporter was expressed to varying degrees in F4/80-expressing ATMs within crown-like structures (**Figure 2a**). GFP expression colocalized with CD11c expression in some, but not all, type 1 ATMs in obese mice (**Figure 2b**). By contrast, colocalization of GFP with $MGL1^+$ type 2 ATMs in epididymal fat was considerably less frequent in obese *$Cx_3cr1^{+/GFP}$* mice (**Figure 2c**). Unexpectedly, we detected clusters of GFP-expressing cells in epididymal fat from both lean (data not shown) and obese *$Cx_3cr1^{+/GFP}$* mice which did not stain strongly for F4/80 (**Figure 2d**). These GFP^+ cells had a unique, dendritic cell-like morphology, and these clusters were often found in hypervascularized areas devoid of adipocytes (**Figure 2d**).

To quantify and further phenotype CX_3CR1-expressing cells in visceral fat, SVCs were isolated from epididymal fat pads of lean and obese *$Cx_3cr1^{+/GFP}$* mice and examined by flow cytometry. Autofluorescence in SVC preparations and the relative infrequency of GFP^+ cells in lean *$Cx_3cr1^{+/GFP}$* mice prevented us from accurately characterizing GFP^+ SVCs in fat from lean reporter mice by this method (data not shown). However, 12 weeks of HFD-induced obesity caused a marked increase in GFP^+ cells in SVC preparations from obese *$Cx_3cr1^{+/GFP}$* mice, which was distinguishable from background autofluorescence (**Figure 3a**). In obese reporter mice, GFP^+ SVCs accounted for ~20% of all SVCs (21.1 ± 06%; $n = 4$ mice) (**Figure 3a**). To determine whether GFP^+ SVCs were ATMs, SVCs were stained for CD11b and F4/80 and divided into $CD11b^{High}F4/80^{High}$

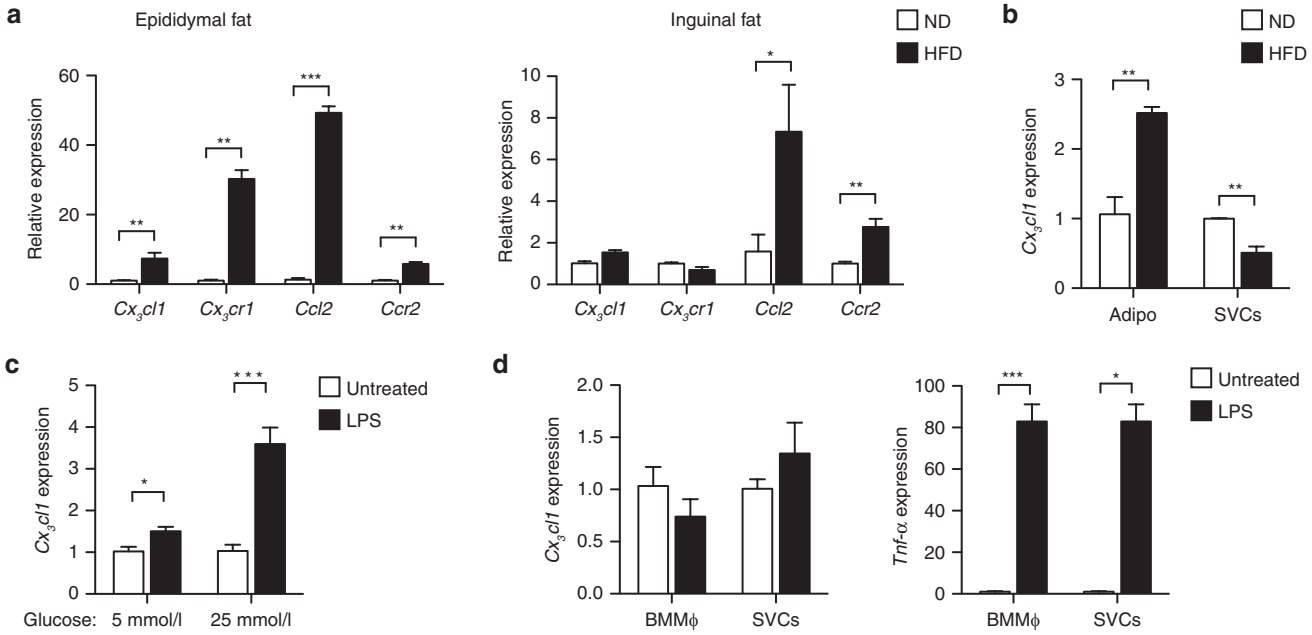

Figure 1 *Cx*$_3$*cl1* and *Cx*$_3$*cr1* expression is increased in epididymal fat during high-fat diet (HFD)-induced obesity in mice. (**a**) Chemokine/receptor gene expression in epididymal (visceral) and inguinal (subcutaneous) adipose tissue from male C57BL/6J mice fed a normal diet (ND; 4.5% fat; $n = 4$) or HFD (60% fat; $n = 4$) for 20 weeks. (**b**) *Cx*$_3$*cl1* expression in isolated adipocytes (Adipo) and stromal vascular cells (SVCs) within epididymal fat pads from ND and HFD mice ($n = 4$ per group). (**c**) *Cx*$_3$*cl1* expression in differentiated 3T3-L1 adipocytes grown in 5 mmol/l and 25 mmol/l glucose and stimulated with lipopolysaccharide (LPS; 100 ng/ml) for 24 h ($n = 3$–4 replicates per treatment). (**d**) *Cx*$_3$*cl1* and *TNF-α* expression in bone marrow-derived macrophages (BMMϕ) and cultured SVCs stimulated with LPS (100 ng/ml) for 24 h ($n = 3$ replicates per treatment). $^*P < 0.05$; $^{**}P < 0.01$; $^{***}P < 0.001$. TNF-α, tumor necrosis factor-α.

(herein defined as ATMs) and CD11b^{High}F4/80^{Low} populations (**Figure 3b**). ATMs and CD11b^{High}F4/80^{Low} SVCs differed in Ly-6c expression and light scatter properties (**Figure 3c**). CD11b^{High}F4/80^{Low} SVCs were Ly-6c^{High}SSC^{Low}FSC^{Mid} suggesting that these cells represent immature myeloid cells (iMCs) in fat. iMCs are unlikely to be residual blood monocytes as the mice in these experiments were perfused with PBS to remove blood before SVC isolation. Notably, GFP$^+$ SVCs made up a larger fraction of the iMCs relative to ATMs (28.08 ± 2.98% ATMs vs. 49.55 ± 3.39% iMCs; $n = 4$ mice) (**Figure 3d**). Consistent with our immunofluorescence studies, quantification revealed that as many as 8% of all SVCs from epididymal fat of obese *Cx*$_3$*cr1*$^{+/GFP}$ mice express GFP, but not F4/80 (8.0 ± 1.76% of total SVCs; $n = 4$ mice). These cells were SSC^{Low} (data not shown), suggesting that they are likely iMCs or an altogether distinct leukocyte subset in visceral fat.

GFP$^+$ ATMs and iMCs from epididymal fat were phenotyped for markers of type 1 (CD11c) and type 2 (CD206) ATMs to determine whether CX$_3$CR1/GFP expression is associated with one or both ATM subtypes. Approximately one quarter of ATMs from epididymal fat were GFP$^+$CD11c$^+$ (26.7 ± 2.14% of ATMs; $n = 4$ mice) and CD11c expression was comparable between GFP$^+$ and GFP$^-$ ATMs collected from *Cx*$_3$*cr1*$^{+/GFP}$ mice after 12 weeks of HFD (**Figure 3f**). By contrast, ~15% of GFP$^+$ ATMs expressed the type 2 ATM marker CD206 (16.0 ± 2.52% of ATMs; $n = 4$ mice). CD206 expression was markedly higher in GFP$^-$ ATMs (**Figure 3f**). This was consistent with our microscopy studies in which we did not observe much colocalization of GFP and MGL1 expression *in situ* (**Figure 2c**). CD11c was also expressed on iMCs from obese reporter mice, and GFP$^+$ CD11c$^+$ iMCs made up about 25% of the total iMC population (27.9 ± 3.47% of total iMCs; $n = 4$ mice)(**Figure 3g**). By contrast, iMCs expressed little CD206 (**Figure 3g**). Taken together, our microscopy and flow cytometry studies demonstrate that CX$_3$CR1 expression is not restricted solely to either type 1 or type 2 ATMs in visceral adipose tissue of mice with HFD-induced obesity. Rather, we identified CX$_3$CR1 expression in both type 1 and type 2 ATMs, as well as a population of CD11c$^+$F4/80^{Low} iMCs.

Cx$_3$*cr1* deficiency in mice does not alter HFD-induced monocytosis

Obesity promotes monocytosis (30,31) and CX$_3$CR1 regulates blood monocyte homeostasis (23). Therefore, we first investigated the impact of *Cx*$_3$*cr1* deficiency on circulating monocytes after short-term (12 weeks) and chronic (40 weeks) exposure to HFD. *Cx*$_3$*cr1*$^{GFP/GFP}$ and littermate control (*Cx*$_3$*cr1*$^{+/GFP}$) mice were fed a HFD for various times (12–40 weeks). *Cx*$_3$*cr1*$^{GFP/GFP}$ and control mice gained weight at a similar rate and developed similar degrees of adiposity in response to HFD-induced obesity (**Supplementary Figure S1** online). The number of circulating CD115$^+$ (Ly-6g$^-$) monocytes in lean *Cx*$_3$*cr1*$^{GFP/GFP}$ mice was significantly reduced compared to control mice (**Figure 4a**), as reported (23). Circulating monocytes were elevated in control mice after chronic (40 weeks), but not short-term (12 weeks) HFD exposure. However, *Cx*$_3$*cr1* deficiency was not sufficient to

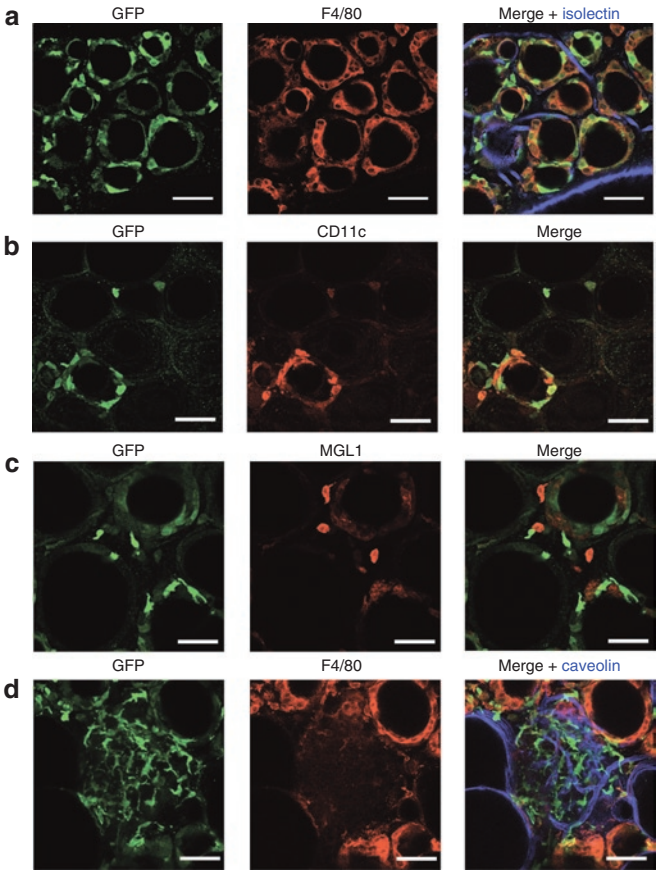

Figure 2 CX_3CR1 is expressed on adipose tissue macrophages (ATMs) in epididymal adipose tissue. (**a**) Identification of GFP$^+$ (green) and F4/80$^+$ (red) ATMs in epididymal fat from obese $Cx_3cr1^{+/GFP}$ reporter mice by confocal microscopy. Isolectin (blue) labels endothelial cells and identifies vasculature. (**b**) GFP$^+$ (green) and CD11c$^+$ (red) type 1 ATMs in epididymal fat. (**c**) GFP$^+$ (green) and MGL1$^+$ (red) type 2 ATMs in epididymal fat. (**d**) Representative image of unique GFP$^+$ (green) cell clusters in hypervascularized regions devoid of adipocytes and F4/80$^+$ (red) ATMs. Caveolin (blue) identifies vasculature. Bar = 100 µm; original magnification = ×60. GFP, green fluorescent protein.

blunt HFD-induced monocytosis as there were no differences in total CD115$^+$ (Ly-6g$^-$) monocytes between obese $Cx_3cr1^{GFP/GFP}$ and control mice (**Figure 4a**). Ly-6c^{Low} monocytes were reduced in lean $Cx_3cr1^{GFP/GFP}$ mice and after 12 weeks of HFD exposure (**Figure 4b,c**). By contrast, Ly-6c^{Low} monocytes were not different in $Cx_3cr1^{GFP/GFP}$ and control mice after 40-weeks of HFD (**Figure 4c**). Relative to control mice, circulating Ly-6c^{High} monocytes were also reduced in lean $Cx_3cr1^{GFP/GFP}$ mice, but no differences in Ly-6c^{High} monocytes were seen between genotypes after short-term or chronic exposure to HFD (**Figure 4d**). When expressed as the relative change from baseline (% of total blood leukocytes in lean mice), $Cx_3cr1^{GFP/GFP}$ mice showed increased monocyte mobilization/stability in the circulation with obesity compared to controls (**Figure 4e**). There results demonstrate that the initiation and maintenance of monocytosis with obesity is independent of CX_3CR1 and implies that HFD-induced obesity activates compensatory mechanisms that overcome monocytopenia caused by Cx_3cr1 deficiency.

Cx_3cr1 deficiency does not alter ATM or iMC content, ATM phenotype, or adipose tissue inflammation in lean or obese mice

To evaluate whether CX_3CR1 plays a role in the recruitment or maintenance of ATMs and/or iMCs in fat, $Cx_3cr1^{GFP/GFP}$ and littermate control mice were fed a HFD for different durations (0, 12, 16, 30, and 40 weeks), and ATM and iMC content in epididymal adipose tissue was examined by flow cytometry. Relative to lean mice, the number of SVCs in epididymal fat increased 3.5- to fourfold following HFD, but there were no differences in the quantity of SVCs in either group of mice at any time point (**Supplementary Figure S2** online). Total ATM content in epididymal fat increased after 12, 16, 30, and 40 weeks of HFD, but there were no differences between obese $Cx_3cr1^{GFP/GFP}$ and control cohorts (**Figure 5a**). The quantity of iMCs decreased in response to HFD; however, we found no differences in iMC content between groups (**Figure 5b**). The number of GFP$^+$ ATMs (CD11b$^+$GFP$^+$ and F4/80$^+$GFP$^+$) in epididymal adipose tissue was also comparable between obese $Cx_3cr1^{GFP/GFP}$ and control mice after 12 weeks of HFD (**Figure 5c**). To rule out the possibility that haploinsufficiency of Cx_3cr1 in obese control ($Cx_3cr1^{GFP/+}$) mice may alter ATM/iMC recruitment, we also compared obese C57BL/6 and $Cx_3cr1^{GFP/GFP}$ mice after 20 weeks of HFD but, again, found no differences in ATM content in epididymal adipose tissue between these two groups (**Figure 5d**).

We next examined the distribution of type 1 and type 2 ATM subtypes in epididymal fat from lean and obese $Cx_3cr1^{GFP/GFP}$ and control mice using multiple techniques. By flow cytometry, type 2 (F4/80$^+$ CD11b$^+$CD206$^+$) ATMs were the predominant ATM subtype in epididymal adipose tissue from both lean $Cx_3cr1^{GFP/GFP}$ and control mice, but these populations were unaffected by Cx_3cr1 deficiency (**Figure 6a**). Twelve weeks of HFD caused an increase in type 1 (F4/80$^+$ CD11b$^+$CD11c$^+$) ATMs in both genotypes; however, the relative numbers of CD11c$^+$ ATMs did not differ between strains (**Figure 6a**). Furthermore, there were no significant differences in the number of CD11c$^-$CD206$^-$ or CD11c$^+$CD206$^+$ ATMs between groups (**Figure 6a**). The ratio of type 1:type 2 ATMs increased to similar levels in both $Cx_3cr1^{GFP/GFP}$ and control mice after 12 weeks of HFD, and this was further exaggerated in mice with chronic obesity (**Figure 6b**). Immunofluorescence microscopy demonstrated that $Cx_3cr1^{GFP/GFP}$ and control mice had similar numbers of Mac2$^+$ crown-like structures in epididymal fat after 12- and 40-weeks of HFD (**Figure 6c** and data not shown), indicating that the absence of CX_3CR1 does not alter the formation of crown-like structures with obesity. Finally, gene expression analysis performed on whole epididymal adipose tissue from obese $Cx_3cr1^{GFP/GFP}$ and control mice did not reveal any significant differences in the expression pattern of M1 or M2 macrophage markers, inflammatory cytokines, or chemokines between the two strains after 12- or 40-weeks of HFD (**Figure 6d,e** and data not shown).

We also examined the effects of Cx_3cr1 deficiency on adipose tissue T lymphocytes implicated in adipose tissue inflammation. By flow cytometry, we detected no significant differences

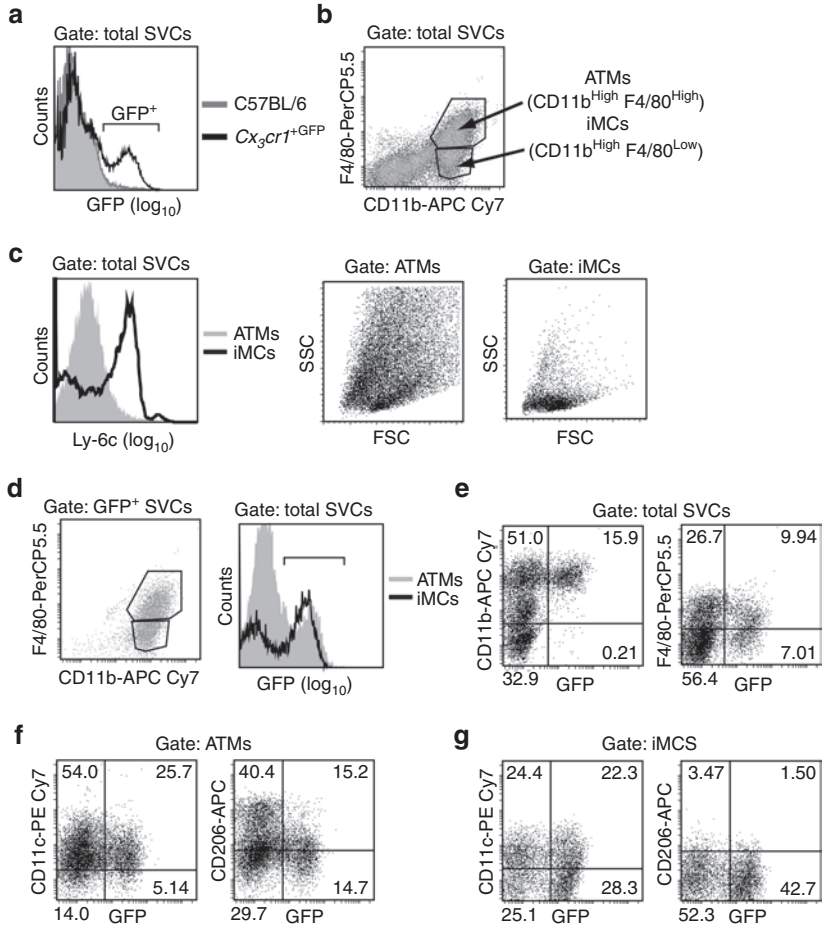

Figure 3 Characterization of CX_3CR1/GFP^+ stromal vascular cells (SVCs) in epididymal adipose tissue of obese *Cx₃cr1*$^{+/GFP}$ mice by flow cytometry. *Cx₃cr1*$^{+/GFP}$ were fed a high-fat diet (HFD; 60% fat) for 12 weeks before SVCs were isolated from epididymal adipose tissue and phenotyped by flow cytometry. (**a**) Identification of GFP^+ SVCs in obese *Cx₃cr1*$^{+/GFP}$ (open) and C57BL/6 (shaded) mice. (**b**) Identification of $CD11b^{High}F4/80^{High}$ (adipose tissue macrophages; ATMs) and $CD11b^{High}F4/80^{Low}$ (immature myeloid cells; iMCs) populations in SVCs from obese mice. (**c**) Representative histogram showing Ly-6c expression in ATMs (shaded) and iMCs (open). Scatter plots (SSC vs. FSC) of gated ATMs (middle) and iMCs (right) demonstrate the difference in cell size and granularity between the two populations. (**d**) Distribution of GFP^+ SVCs from a representative obese *Cx₃cr1*$^{+/GFP}$ mouse. GFP expression in ATMs and iMCS is shown. (**e**) Representative scatter plots showing $CD11b^+GFP^-$ and $CD11b^+GFP^+$ SVCs (left) and $F4/80^+GFP^-$ and $F4/80^+GFP^+$ SVCs (right) within visceral fat from obese *Cx₃cr1*$^{+/GFP}$ mice. (**f**) $CD11c^+GFP^-$ and $CD11c^+GFP^+$ ATMs (left) and $CD206^+GFP^-$ and $CD206^+GFP^+$ ATMs (right) within visceral fat from obese *Cx₃cr1*$^{+/GFP}$ mice. (**g**) $CD11c^+GFP^-$ and $CD11c^+GFP^+$ iMCs (left) and $CD206^+GFP^-$ and $CD206^+GFP^+$ iMCs (right) within visceral fat from from obese *Cx₃cr1*$^{+/GFP}$ mice. In **e**–**g**, percentage of gated cells is indicated in each quadrant. APC, allophycocyanin; FSC, forward scatter; GFP, green fluorescent protein; PE, R-phycoerythrin; SSC, side scatter.

in the number of $CD4^+$ or $CD8^+$ T cells within epididymal adipose tissue when comparing obese *Cx₃cr1*$^{GFP/GFP}$ and control mice (**Supplementary Figure S3** online). Collectively, these data indicate that CX_3CR1 expression is not required for the recruitment, turnover, or retention of ATMs or T lymphocytes in visceral adipose tissue during HFD.

Disruption of Cx_3cr1 does not impact the development of obesity-induced metabolic disease in mice

Since it is plausible that *Cx₃cr1* deficiency may augment HFD-induced metabolic disease without affecting obesity-induced inflammation in fat, we evaluated glucose metabolism, insulin sensitivity, and hepatic triglyceride content in lean and obese *Cx₃cr1*$^{GFP/GFP}$ and control $Cx_3cr1^{GFP/+}$ mice. *Cx₃cr1*$^{GFP/GFP}$ and control mice developed similar degrees of hyperglycemia and hyperinsulinemia during HFD-induced obesity (**Figure 7a**). Glucose and insulin tolerance tests performed after 23 weeks of HFD-induced obesity confirmed that, compared to lean controls, obese *Cx₃cr1*$^{GFP/GFP}$ and control mice had similar impairments in glucose tolerance (**Figure 7b**) and insulin sensitivity (**Figure 7c**). A independent cohort of $Cx_3cr1^{GFP/GFP}$ mice was also indistinguishable from age-matched $Cx_3cr1^{+/+}$ mice in terms of HFD-induced insulin resistance (**Supplementary Figure S4** online). *Cx₃cr1*$^{GFP/GFP}$ and $Cx_3cr1^{GFP/+}$ control mice developed similar degrees of liver steatosis in response to HFD (**Figure 7d,e**). This latter finding indicates that CX_3CR1 is not required for (or protective against) HFD-induced steatosis in mice.

DISCUSSION

In this study, we examined the hypothesis that the chemokine receptor CX_3CR1 plays a role in the regulation of monocyte

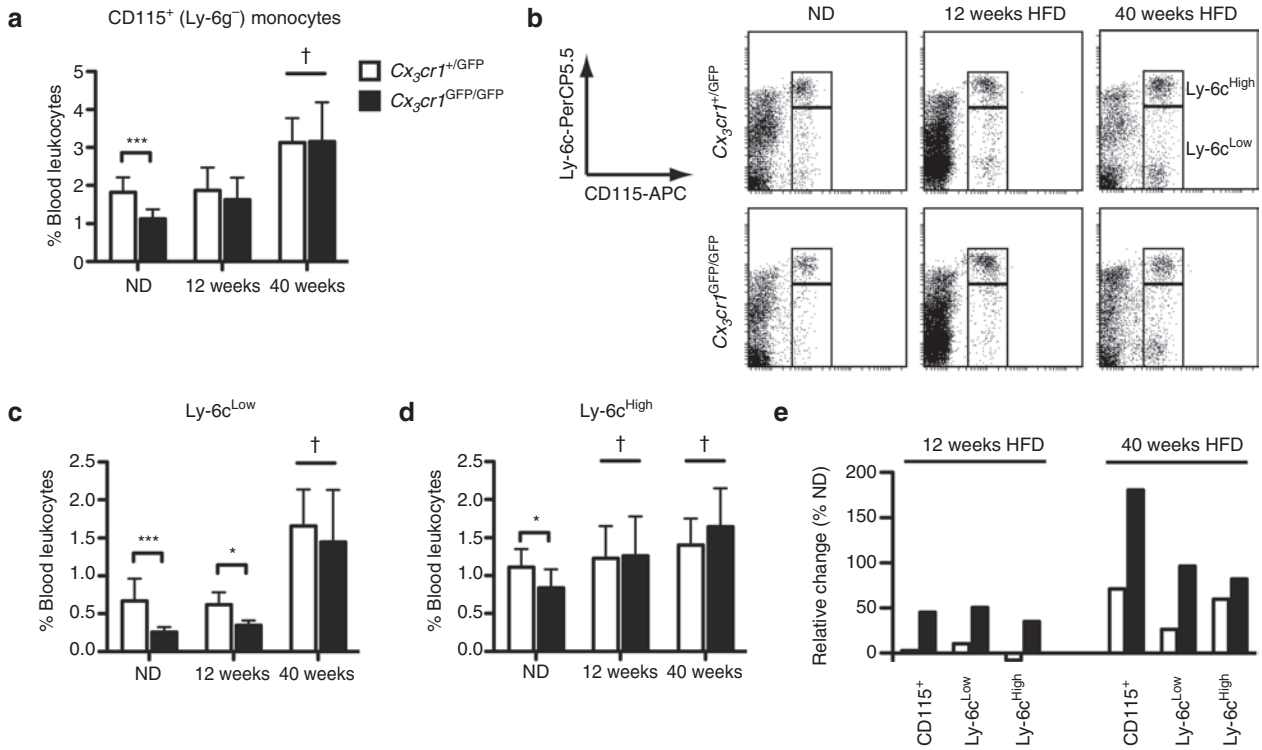

Figure 4 Effects of high-fat diet (HFD)-induced obesity on blood monocyte populations in $Cx_3cr1^{GFP/GFP}$ and control mice. $Cx_3cr1^{+/GFP}$ and $Cx_3cr1^{GFP/GFP}$ mice were fed a normal diet (ND) or HFD (60% fat) for 12 or 40 weeks before blood leukocytes were examined by flow cytometry. (**a**) Total circulating CD115$^+$ Ly-6g$^-$ monocytes in $Cx_3cr1^{+/GFP}$ and $Cx_3cr1^{GFP/GFP}$ mice. (**b**) Representative scatter plots showing the distribution of blood monocyte subsets (Ly-6c^{High} and Ly-6c^{Low}) from lean (ND) and obese (12- and 40-weeks HFD) mice. (**c**,**d**) Quantification of blood monocyte subsets after gating Ly-6c^{High} and Ly-6c^{Low} populations as indicated in **b**. (**e**) Relative change in blood monocytes in $Cx_3cr1^{+/GFP}$ and $Cx_3cr1^{GFP/GFP}$ mice with HFD-induced obesity. Data are expressed as percentage of total blood leukocytes from lean mice. n = 5–8 per group; $^*P < 0.05$; $^{***}P < 0.001$; $^{\dagger}P < 0.05$ vs. ND. GFP, green fluorescent protein.

trafficking to adipose tissue during HFD-induced obesity. Support for this hypothesis came from the recent observation that plasma and adipose tissue levels of fractalkine/CX_3CL1, the only ligand for CX_3CR1, are elevated in obese patients (29). We found that hyperglycemia synergizes with inflammatory signals to promote Cx_3cl1 expression in cultured adipocytes and that HFD-induced obesity induces Cx_3cr1 expression in adipocytes in visceral, but not subcutaneous fat. However, we found no significant alterations in ATM accumulation, inflammatory capacity, or insulin resistance in lean or obese Cx_3cr1^- deficient mice.

Using $Cx_3cr1^{+/GFP}$ reporter mice, we found that CX_3CR1 was expressed on both type 1 and type 2 ATMs identified by surface marker staining for CD11c and CD206/MGL1, respectively, in both lean and obese mice. However, CX_3CR1/GFP was not preferentially expressed in either type 1 (CD11c$^+$) or type 2 (CD206$^+$/MGL1$^+$) ATMs. Moreover, Cx_3cr1 deficiency did not the affect the accumulation of GFP$^+$ myeloid cells in fat during diet-induced obesity or alter the recruitment of type 1 ATMs to visceral fat. However, CX_3CR1/GFP expression did identify a population of cells *in situ* that morphologically resemble CX_3CR1^+ dendritic cells in the gut (32). Located in hypervascular regions in visceral fat, these cell clusters appear to be synonymous with fat-associated lymphoid clusters identified in mesenteric fat (33). Thus, $Cx_3cr1^{+/GFP}$ reporter mice have utility in the identification of fat-associated lymphoid clusters in visceral fat in both lean and obese states.

CX_3CR1/GFP expression was not confined to ATMs in epididymal fat. About half of GFP$^+$ CD11b$^+$ SVCs in visceral fat were smaller and less granular (FSC^{mid} SSC^{low}) and expressed lower levels of F4/80 than ATMs. These cells are similar to F4/80^{Low} SVCs previously reported in visceral fat from mice (34,35). Like iMCs, F4/80^{Low} SVCs decline progressively with diet-induced obesity (35). Notably, F4/80^{Low} SVCs express higher levels of *Nos2*, *Ccl5*, and *Csf1* (macrophage colony-stimulating factor) than F4/80^{High} ATMs (35), suggesting that F4/80^{Low} SVCs may be a unique reservoir of inflammatory myeloid cells. In our study, the surface phenotype of iMCs (Ly-6c^{High}, CD11c$^+$, CD206$^-$) suggests that these cells may be analogous to classical (Ly6c^{High}) blood monocytes in the circulation; however, these cells were not dissociated from visceral fat by saline perfusion, suggesting that iMCs are tissue resident "monocyte-like" cells intimately associated with adipocytes or the vasculature within the tissue. The expression of CD11c by iMCs raises the possibility that they may be precursors of CD11c$^+$ inflammatory (M1) ATMs. We speculate that obesity accelerates the transition of iMCs from a "monocyte-like" phenotype to a "macrophage-like" state. However, detailed fate mapping studies will be required to prove this and to establish the role of these cells in adipose tissue inflammation.

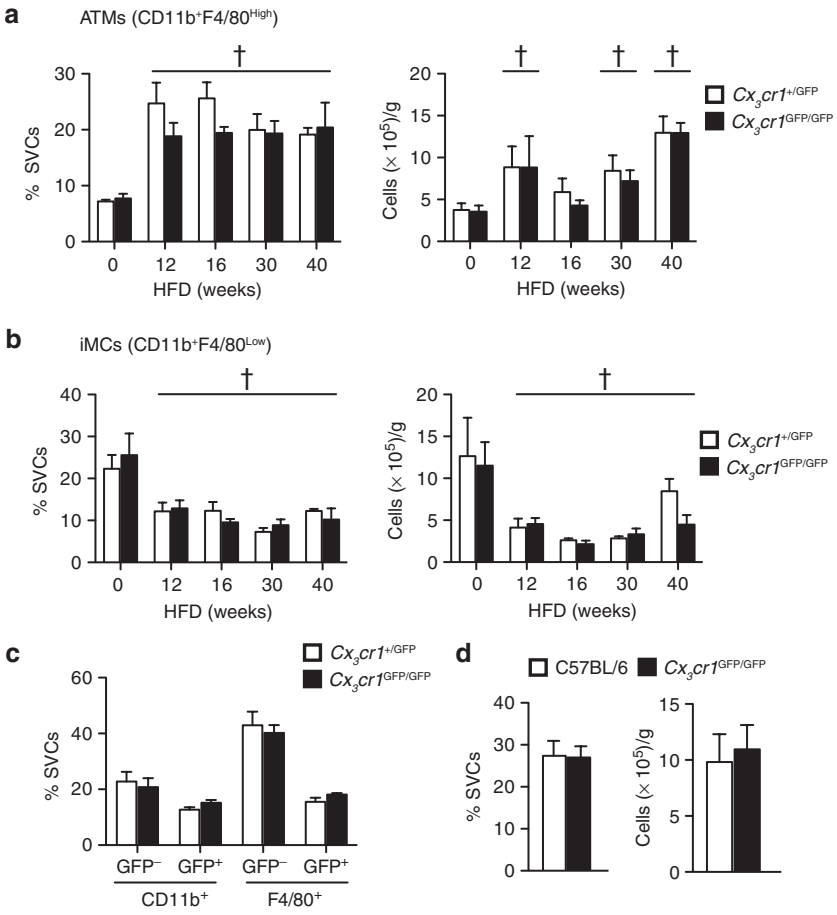

Figure 5 *Cx$_3$cr1* deficiency does not alter adipose tissue macrophage (ATM) content in visceral fat from lean or obese mice. *Cx$_3$cr1*$^{+/GFP}$ and *Cx$_3$cr1*$^{GFP/GFP}$ mice were fed a normal diet (ND) or high-fat diet (HFD) for 12, 16, 30 or 40 weeks before stromal vascular cells (SVCs) were isolated from epididymal adipose tissue and examined by flow cytometry. (**a**) ATM content in epididymal fat shown as percentage of total SVCs and normalized to visceral fat mass. (**b**) Immature myeloid cell (iMC) content in epididymal fat shown as percentage of total SVCs and normalized to visceral fat mass. (**c**) Distribution of GFP$^+$ and GFP$^-$ SVCs in visceral fat after 12 weeks of HFD. Data are shown as percentage of total SVCs. (**d**) ATM content in visceral fat from C57BL/6 and *Cx$_3$cr1*$^{GFP/GFP}$ mice after 20 weeks of HFD. Data are shown as percentage of total SVCs and normalized to visceral fat mass. ND: $n = 4$ per group; HFD: $n = 4$–5 per group; $^{\dagger}P < 0.05$ vs. ND. GFP, green fluorescent protein.

Atherosclerosis and obesity-induced adipose tissue inflammation are very similar inflammatory diseases, with many of the same inflammatory mediators (e.g., monocytes, macrophages, dendritic cells, T cells, B cells, etc.) (11,12). Currently, it is largely assumed that leukocyte trafficking to atherosclerotic plaques and trafficking of leukocytes to obese adipose tissue is regulated by a similar set of chemokine signals (e.g., CCL2/CCR2 and CX$_3$CL1/CX$_3$CR1). Why then does disruption of the CX$_3$CL1-CX$_3$CR1 pathway attenuate foam cell formation in atherosclerotic vessels, but does not impact ATM accumulation in mouse models of diet-induced obesity? Several differences potentially exist in mice models of these two diseases that may explain why CX$_3$CR1 is required for one process but not the other.

Monocytosis is a hallmark of murine models of atherosclerosis and diet-induced obesity. Classical (Ly-6c^{High}) and nonclassical (Ly-6c^{Low}) blood monocytes are elevated in *Apoe*$^{-/-}$ mice (14,27). CX$_3$CR1 is required for the trafficking of Ly-6c^{High} monocytes to atherosclerotic lesions (14,22) and the CX$_3$CL1-CX$_3$CR1 pathway also promotes survival of Ly-6c^{Low} monocytes (23). Thus, *Cx3cr1*$^{-/-}$*Apoe*$^{-/-}$ mice are protected from atherogenesis due to a combination of defective monocyte trafficking and impaired monocyte survival. By contrast, classical (Ly-6c^{High}) blood monocytes as well as CD11c$^+$ monocytes are elevated in mouse models of obesity (31). The importance of Ly-6c^{High} blood monocytes in the progression of HFD-induced inflammation in fat and metabolic disease is underscored by studies showing that type 1 ATM accumulation, inflammation, and metabolic disease are all attenuated in obese *Ccr2*$^{-/-}$ and *Mgl1*$^{-/-}$ mice that have few circulating Ly-6c^{High} monocytes (4–5,15). In our experiments, both Ly-6c^{High} and Ly-6c^{Low} blood monocytes increased with HFD-induced obesity, but these increases were not dependent on CX$_3$CR1. Ly-6c^{Low} blood monocytes were reduced after 12 weeks of HFD in *Cx$_3$cr1*$^{GFP/GFP}$ mice, suggesting that CX$_3$CR1 is required for their survival in diet-induced obesity. However, reduced Ly-6c^{Low} monocytes did not alter ATM accumulation in epididymal fat from obese *Cx$_3$cr1*$^{GFP/GFP}$ mice, suggesting that nonclassical monocytes likely contribute little to the obesity-induced accumulation of type 1 ATMs in visceral fat. These findings highlight the need for a more sophisticated understanding

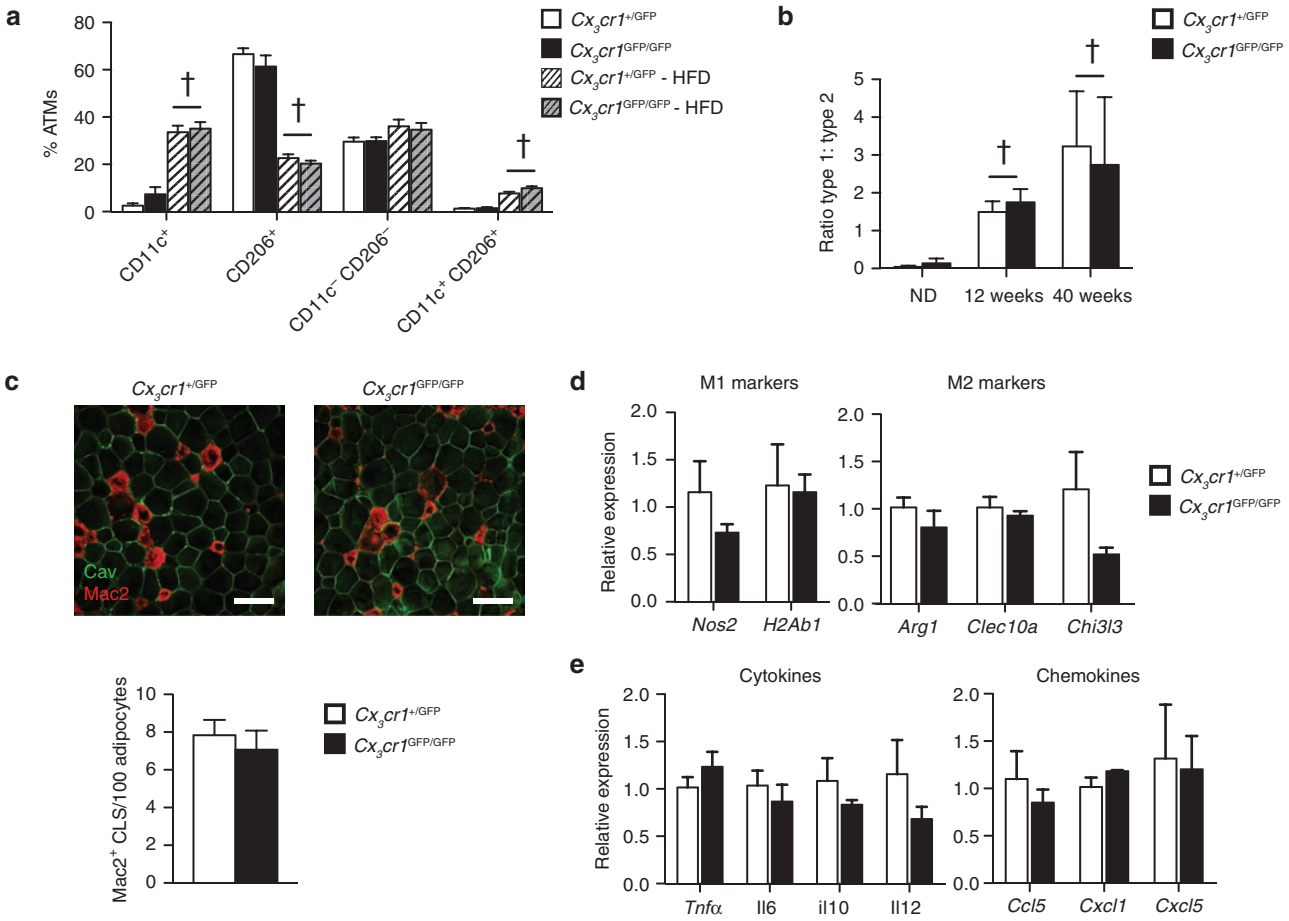

Figure 6 *Cx$_3$cr1* deficiency does not alter the distribution of type 1 and type 2 adipose tissue macrophages (ATMs) in epididymal adipose tissue from lean or obese mice. *Cx$_3$cr1*$^{+/GFP}$ and *Cx$_3$cr1*$^{GFP/GFP}$ mice were fed a normal diet (ND) or high-fat diet (HFD) for 12 weeks before stromal vascular cells (SVCs) were isolated from epididymal fat and examined by flow cytometry. (**a**) Distribution of ATM subsets in visceral fat from *Cx$_3$cr1*$^{+/GFP}$ and *Cx$_3$cr1*$^{GFP/GFP}$ mice shown as percentage of total ATMs. (**b**) Ratio of type 1 (CD11c$^+$) to type 2 (CD206$^+$) ATMs in visceral fat after 12- and 40-weeks of HFD. (**c**) ATM infiltration assessed by immunofluorescence microscopy. Caveolin (green) and Mac2 (red) staining in epididymal fat from obese (12 weeks HFD) mice. Bar = 100 µm. (**d**) Relative expression of M1 and M2 macrophage markers in visceral fat from *Cx$_3$cr1*$^{+/GFP}$ and *Cx$_3$cr1*$^{GFP/GFP}$ mice after 12 weeks of HFD. (**e**) Relative expression of a subset of cytokines and chemokines in epididymal fat after 12 weeks of HFD. n = 4–5 mice per group. $^{\dagger}P < 0.05$ vs. ND. CLS, crown-like structures; GFP, green fluorescent protein.

of the mechanisms that guide and sustain monocyte egress from bone marrow and splenic reservoirs during diet-induced obesity in mice models.

The development of atherosclerosis and adipose tissue inflammation with obesity have been shown to be dependent upon the CCR2 (13–16). Like our current study, others have reported that chemokines known to be involved in atherogenesis (e.g., CCL2, MIP-1α/CCL3) are induced in obese visceral fat (36,37). However, genetic disruption of many of these chemokines does not attenuate the accumulation of inflammatory ATMs in HFD-fed mice (36,37). This suggests that there is considerable redundancy in chemotaxic signals that drive monocyte trafficking to fat. Alternatively, chemokine-independent signals (e.g., lipolysis, ref. (38)) may play an important role in mediating ATM recruitment to visceral fat, at least in mice models. Clearly, additional work is needed to clarify the importance of chemokine-dependent and -independent signals in the regulation of leukocyte trafficking to fat.

Monocyte extravasation into damaged tissues requires chemoattraction, rolling adhesion, arrest/tight adhesion, and endothelial transmigration. The CX_3CL1/CX_3CR1 interaction is critical for monocyte extravasation in atherosclerotic vessels due in part to the ability of fractalkine/CX_3CL1 to act as an adhesion molecule (14,22). At present, very little is known about how monocyte extravasation occurs in lean and obese fat. The frequency of slow rolling leukocytes in adipose tissue vasculature increases during obesity, and intercellular adhesion molecule-dependent arrest/adhesion of leukocytes has been documented in blood vessels within adipose tissue from obese mice (39). However, it is not known which other adhesion molecules are required or sufficient to promote leukocyte entry into fat. Our results suggest that CX_3CL1/CX_3CR1 pathway is dispensable for monocyte extravasation into fat. Thus, the function of CX_3CL1–CX_3CR1 interactions in the process of monocyte diapedesis may not be conserved in all tissues.

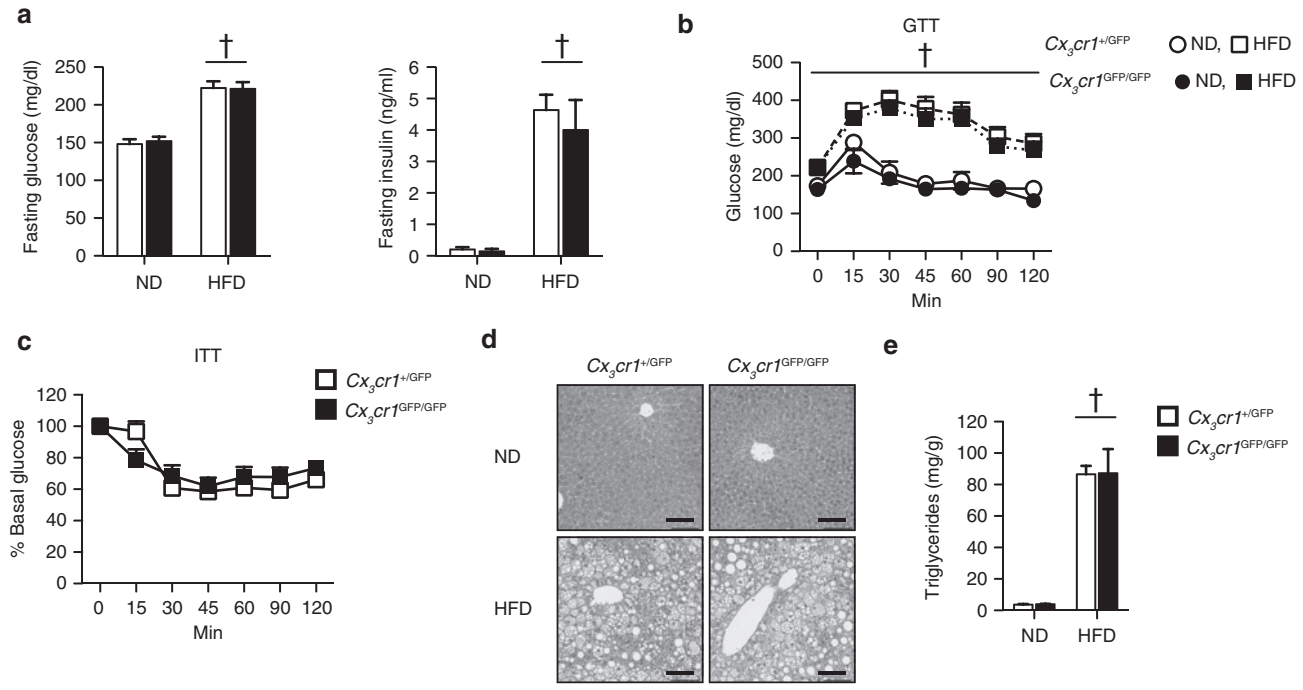

Figure 7 *Cx$_3$cr1* deficiency does not prevent diet-induced metabolic disease. (**a**) Fasting (6 h) glucose and insulin levels lean *Cx$_3$cr1*$^{+/GFP}$ and *Cx$_3$cr1*$^{GFP/GFP}$ mice and after 23 weeks of high-fat diet (HFD)-induced obesity (n = 8–10 per group). (**b**) Glucose tolerance tests (GTT) performed in obese *Cx$_3$cr1*$^{+/GFP}$ and *Cx$_3$cr1*$^{GFP/GFP}$ mice after 23 weeks of HFD (n = 12–13 per group). GTT curves for lean (ND) mice (n = 3–4 per group) are shown (circles) for comparison. (**c**) Insulin tolerance tests (ITT) were performed on *Cx$_3$cr1*$^{+/GFP}$ and *Cx$_3$cr1*$^{GFP/GFP}$ mice (n = 12–13 per group) after 29 weeks of HFD. Data is expressed as % of initial blood glucose levels. (**d**) Representative hematoxylin and eosin-stained sections of liver biopsies from lean and obese (30 weeks HFD) *Cx$_3$cr1*$^{+/GFP}$ and *Cx$_3$cr1*$^{GFP/GFP}$ mice. Bar = 200 µm. (**e**) Liver triglyceride content in lean and obese *Cx$_3$cr1*$^{+/GFP}$ and *Cx$_3$cr1*$^{GFP/GFP}$ mice (n = 4 per group). $^{\dagger}P < 0.05$ vs. ND. GFP, green fluorescent protein; ND, normal diet.

Atherosclerosis and obesity are similar in that they are lipid storage diseases, but there are notable differences between mouse models of atherosclerosis (e.g., *Apoe*$^{-/-}$ mice) and mice with HFD-induced obesity. For one, *Apoe*$^{-/-}$ mice remain more insulin sensitive than wild-type mice when both are fed modest 20% fat diets (40). By contrast, recombinant adiponectin attenuates inflammation and improves insulin sensitivity in mice with HFD-induced obesity, but is unable to modify atherosclerosis progression in *Apoe*$^{-/-}$ mice (41). These findings, coupled to the our findings that CX_3CR1 is not required for ATM recruitment, highlight a critical point of divergence between the mechanisms that regulate foam cell formation in atherosclerosis and ATM accumulation with obesity. Thus, the idea that the factors that regulate foam cell formation during atherogenesis are synonymous with those that promote ATM accumulation in obesity needs to be revisited to provide opportunities for new mechanisms of monocyte trafficking to be discovered.

SUPPLEMENTARY MATERIAL

Supplementary material is linked to the online version of the paper at http://www.nature.com/oby

ACKNOWLEDGMENTS

We thank Lynn Geletka, Kanakadurga Singer, and Kaewon Cho for technical assistance and helpful discussion. This study was supported by NIH grants DK090262 and DK078851 (to C.N.L.). D.L.M. is supported by an NIH NRSA award (DK091976).

DISCLOSURE

The authors declared no conflict of interest.

REFERENCES

1. Hotamisligil GS. Inflammation and metabolic disorders. *Nature* 2006;444:860–867.
2. Olefsky JM, Glass CK. Macrophages, inflammation, and insulin resistance. *Annu Rev Physiol* 2010;72:219–246.
3. Zeyda M, Farmer D, Todoric J *et al*. Human adipose tissue macrophages are of an anti-inflammatory phenotype but capable of excessive pro-inflammatory mediator production. *Int J Obes (Lond)* 2007;31:1420–1428.
4. Westcott DJ, Delproposto JB, Geletka LM *et al*. MGL1 promotes adipose tissue inflammation and insulin resistance by regulating 7/4hi monocytes in obesity. *J Exp Med* 2009;206:3143–3156.
5. Lumeng CN, Bodzin JL, Saltiel AR. Obesity induces a phenotypic switch in adipose tissue macrophage polarization. *J Clin Invest* 2007;117:175–184.
6. Xu H, Barnes GT, Yang Q *et al*. Chronic inflammation in fat plays a crucial role in the development of obesity-related insulin resistance. *J Clin Invest* 2003;112:1821–1830.
7. Weisberg SP, McCann D, Desai M *et al*. Obesity is associated with macrophage accumulation in adipose tissue. *J Clin Invest* 2003;112:1796–1808.
8. Lumeng CN, DelProposto JB, Westcott DJ, Saltiel AR. Phenotypic switching of adipose tissue macrophages with obesity is generated by spatiotemporal differences in macrophage subtypes. *Diabetes* 2008;57:3239–3246.
9. Strissel KJ, Stancheva Z, Miyoshi H *et al*. Adipocyte death, adipose tissue remodeling, and obesity complications. *Diabetes* 2007;56:2910–2918.
10. Patsouris D, Li PP, Thapar D *et al*. Ablation of CD11c-positive cells normalizes insulin sensitivity in obese insulin resistant animals. *Cell Metab* 2008;8:301–309.
11. Surmi BK, Hasty AH. The role of chemokines in recruitment of immune cells to the artery wall and adipose tissue. *Vascul Pharmacol* 2010;52:27–36.

12. Gordon S. Macrophage heterogeneity and tissue lipids. *J Clin Invest* 2007;117:89–93.
13. Ito A, Suganami T, Yamauchi A *et al*. Role of CC chemokine receptor 2 in bone marrow cells in the recruitment of macrophages into obese adipose tissue. *J Biol Chem* 2008;283:35715–35723.
14. Tacke F, Alvarez D, Kaplan TJ *et al*. Monocyte subsets differentially employ CCR2, CCR5, and CX3CR1 to accumulate within atherosclerotic plaques. *J Clin Invest* 2007;117:185–194.
15. Weisberg SP, Hunter D, Huber R *et al*. CCR2 modulates inflammatory and metabolic effects of high-fat feeding. *J Clin Invest* 2006;116:115–124.
16. Kanda H, Tateya S, Tamori Y *et al*. MCP-1 contributes to macrophage infiltration into adipose tissue, insulin resistance, and hepatic steatosis in obesity. *J Clin Invest* 2006;116:1494–1505.
17. Liu J, Divoux A, Sun J *et al*. Genetic deficiency and pharmacological stabilization of mast cells reduce diet-induced obesity and diabetes in mice. *Nat Med* 2009;15:940–945.
18. Winer S, Chan Y, Paltser G *et al*. Normalization of obesity-associated insulin resistance through immunotherapy. *Nat Med* 2009;15:921–929.
19. Winer DA, Winer S, Shen L *et al*. B cells promote insulin resistance through modulation of T cells and production of pathogenic IgG antibodies. *Nat Med* 2011;17:610–617.
20. Geissmann F, Auffray C, Palframan R *et al*. Blood monocytes: distinct subsets, how they relate to dendritic cells, and their possible roles in the regulation of T-cell responses. *Immunol Cell Biol* 2008;86:398–408.
21. Geissmann F, Jung S, Littman DR. Blood monocytes consist of two principal subsets with distinct migratory properties. *Immunity* 2003;19:71–82.
22. Imai T, Hieshima K, Haskell C *et al*. Identification and molecular characterization of fractalkine receptor CX3CR1, which mediates both leukocyte migration and adhesion. *Cell* 1997;91:521–530.
23. Landsman L, Bar-On L, Zernecke A *et al*. CX3CR1 is required for monocyte homeostasis and atherogenesis by promoting cell survival. *Blood* 2009;113:963–972.
24. Lesnik P, Haskell CA, Charo IF. Decreased atherosclerosis in CX3CR1-/- mice reveals a role for fractalkine in atherogenesis. *J Clin Invest* 2003;111:333–340.
25. Teupser D, Pavlides S, Tan M *et al*. Major reduction of atherosclerosis in fractalkine (CX3CL1)-deficient mice is at the brachiocephalic artery, not the aortic root. *Proc Natl Acad Sci USA* 2004;101:17795–17800.
26. Liu P, Yu YR, Spencer JA *et al*. CX3CR1 deficiency impairs dendritic cell accumulation in arterial intima and reduces atherosclerotic burden. *Arterioscler Thromb Vasc Biol* 2008;28:243–250.
27. Combadière C, Potteaux S, Rodero M *et al*. Combined inhibition of CCL2, CX3CR1, and CCR5 abrogates Ly6C(hi) and Ly6C(lo) monocytosis and almost abolishes atherosclerosis in hypercholesterolemic mice. *Circulation* 2008;117:1649–1657.
28. Saederup N, Chan L, Lira SA, Charo IF. Fractalkine deficiency markedly reduces macrophage accumulation and atherosclerotic lesion formation in CCR2-/- mice: evidence for independent chemokine functions in atherogenesis. *Circulation* 2008;117:1642–1648.
29. Shah R, Hinkle CC, Ferguson JF *et al*. Fractalkine is a novel human adipochemokine associated with type 2 diabetes. *Diabetes* 2011;60:1512–1518.
30. Boschmann M, Engeli S, Adams F *et al*. Adipose tissue metabolism and CD11b expression on monocytes in obese hypertensives. *Hypertension* 2005;46:130–136.
31. Wu H, Perrard XD, Wang Q *et al*. CD11c expression in adipose tissue and blood and its role in diet-induced obesity. *Arterioscler Thromb Vasc Biol* 2010;30:186–192.
32. Schulz O, Jaensson E, Persson EK *et al*. Intestinal CD103+, but not CX3CR1+, antigen sampling cells migrate in lymph and serve classical dendritic cell functions. *J Exp Med* 2009;206:3101–3114.
33. Moro K, Yamada T, Tanabe M *et al*. Innate production of T(H)2 cytokines by adipose tissue-associated c-Kit(+)Sca-1(+) lymphoid cells. *Nature* 2010;463:540–544.
34. Bassaganya-Riera J, Misyak S, Guri AJ, Hontecillas R. PPAR gamma is highly expressed in F4/80(hi) adipose tissue macrophages and dampens adipose-tissue inflammation. *Cell Immunol* 2009;258:138–146.
35. Gutierrez DA, Kennedy A, Orr JS *et al*. Aberrant accumulation of undifferentiated myeloid cells in the adipose tissue of CCR2-deficient mice delays improvements in insulin sensitivity. *Diabetes* 2011;60:2820–2829.
36. Kirk EA, Sagawa ZK, McDonald TO, O'Brien KD, Heinecke JW. Monocyte chemoattractant protein deficiency fails to restrain macrophage infiltration into adipose tissue [corrected]. *Diabetes* 2008;57:1254–1261.
37. Surmi BK, Webb CD, Ristau AC, Hasty AH. Absence of macrophage inflammatory protein-1{alpha} does not impact macrophage accumulation in adipose tissue of diet-induced obese mice. *Am J Physiol Endocrinol Metab* 2010;299:E437–E445.
38. Kosteli A, Sugaru E, Haemmerle G *et al*. Weight loss and lipolysis promote a dynamic immune response in murine adipose tissue. *J Clin Invest* 2010;120:3466–3479.
39. Nishimura S, Manabe I, Nagasaki M *et al*. *In vivo* imaging in mice reveals local cell dynamics and inflammation in obese adipose tissue. *J Clin Invest* 2008;118:710–721.
40. Kawashima Y, Chen J, Sun H *et al*. Apolipoprotein E deficiency abrogates insulin resistance in a mouse model of type 2 diabetes mellitus. *Diabetologia* 2009;52:1434–1441.
41. Nawrocki AR, Hofmann SM, Teupser D *et al*. Lack of association between adiponectin levels and atherosclerosis in mice. *Arterioscler Thromb Vasc Biol* 2010;30:1159–1165.